

Accuracy of the semiclassical picture of photoionization in intense laser fields

Li Guo¹, Shilin Hu², Mingqing Liu^{3,4}, Zheng Shu^{3,4}, XiWang Liu⁵, Jie Li⁵, Weifeng Yang⁵, Ronghua Lu¹, ShenSheng Han^{1,†}, and Jing Chen^{2,3,‡}

¹ Key laboratory for Quantum Optics and Center for Cold Atom Physics,
Shanghai Institute of Optics and Fine Mechanics,
Chinese Academy of Sciences, Shanghai 201800, China

² Laboratory of Quantum Engineering and Quantum Metrology, School of Physics and Astronomy,
Sun Yat-Sen University (Zhuhai Campus), Zhuhai 519082, China

³ HEDPS, Center for Applied Physics and Technology,
Collaborative Innovation Center of IFSA, Peking University, Beijing 100084, China

⁴ Institute of Applied Physics and Computational Mathematics, P. O. Box 8009, Beijing 100088, China and

⁵ Department of Physics, College of Science, Shantou University, Shantou, Guangdong 515063, China

In the semiclassical picture of photoionization process in intense laser fields, the ionization rate solely depends on the amplitude of the electric field and the final photoelectron momentum corresponds to the instant of ionization of the photoelectron, however, this picture has never been checked rigorously. Recently an attosecond angular streaking technique based on this semiclassical perspective has been widely applied to temporal measurement of the atomic and molecular dynamics in intense laser fields. We use a Wigner-distribution-like function to calculate the time-emission angle distribution, angular distribution and ionization time distribution for atomic ionization process in elliptically polarized few-cycle laser fields. By comparing with semiclassical calculations, we find that the two methods always show discrepancies except in some specific cases and the offset angles are generally not consistent with the offset times of the ionization time distributions obtained by the two methods even when the non-adiabatic effect is taken into account, indicating that the “attoclock” technique is in principle inaccurate. Moreover, calculations for linearly polarized laser fields also show similar discrepancies between two methods in the ionization time distribution. Our analysis indicates that the discrepancy between the semiclassical and quantum calculations can be attributed to correlation, i. e., temporal nonlocalization effect.

PACS numbers: 32.80.Rm; 32.80.Fb

INTRODUCTION

Study on above-threshold ionization (ATI) plays an essential role in our comprehension of various phenomena in strong-field atomic physics [1, 2]. So far, a categorization of the ionization process has been widely accepted: two distinct regimes- multiphoton ionization and tunneling ionization are distinguished by the Keldysh parameter $\gamma = \sqrt{\frac{I_p}{2U_p}}$ with $\gamma \ll 1$ for tunneling ionization and $\gamma \gg 1$ for multiphoton ionization [3]. Here, I_p is the ionization potential of the atom and U_p is the ponderomotive energy. In the multiphoton regime, the ionization occurs via absorption of n photons from the field. In the tunneling regime, the electron is considered to tunnel through the barrier created by the superposition of the laser field and Coulomb potential and thereafter can be treated as a free electron evolving in the external laser field. This is commonly known as the simpleman’s picture of the ATI process [4], which comprises the picture to understand atomic and molecular dynamics in intense laser fields [2, 5] and constitutes the foundation of attosecond

measurement [6].

In this semiclassical picture, the ionization rate of the electron is only determined by the instantaneous amplitude of the laser field and the final photoelectron momentum is equal to the vector potential of the laser field at the ionization moment with opposite sign if the influence of the ionic potential is ignored, however, this correspondence, or the accuracy of the semiclassical approximation of the photoionization process, has never been rigorously checked, or in other words, how accurate the semiclassical picture is still remains an open question. Recently, an attosecond angular streaking technique, also dubbed as “attoclock” technique, has been developed to investigate the temporal dynamics of atoms and molecules in intense laser fields [7–13]. This technique, different from the conventional attosecond measurement which relies on attosecond pulses generated using high-order harmonic generation process and is very technically demanding, uses the rotating electric-field vector of an intense close-to-circularly polarized pulse to deflect photo-ionized electrons in the radial spatial direction. Then the instant of ionization is mapped to the final angle of the momentum vector in the polarization plane according to the semiclassical picture. When a few-cycle pulse is applied, a comparison between the peaks of the measured photoelectron angular distribution and the simpleman’s prediction shows an offset angle which has caused much

[†] sshan@mail.shcnc.ac.cn

[‡] chen_jing@iapcm.ac.cn

debate on its underlying mechanism [8, 10, 11, 13, 14]. Ionic Coulomb potential, tunneling time delay and nonadiabatic effect have been proposed to explain this offset angle. By comparing the experimental data with the semiclassical calculation including the Coulomb potential, Eckle *et al.* place an intensity-averaged upper limit of 12 attoseconds on the tunneling delay time in strong field ionization of a helium atom [8]. Boge *et al.* find that the nonadiabatic effect is unimportant [11]. However, by solving a three-dimensional time-dependent Schrödinger equation, Ivanov *et al.* [14] give an opposite view against the calculations using the semiclassical model [11]. Recently, Torlina *et al.* show that the offset angle can be attributed to the Coulomb potential effect and confirm the zero tunneling time delay by theoretical calculation [15].

It is noteworthy that the principle of the attosecond streaking technique, viz., the angle of the final momentum vector corresponds to the instant of the tunneling ionization, is based on the semiclassical picture. Therefore, prior to consideration of the Coulomb potential and nonadiabatic effects *etc.* [8, 16–23], one needs to rigorously check the principle of the attoclock technique, or the accuracy of the semiclassical picture in description of the photoionization process which is an intrinsic quantum process.

In this paper, we use a Wigner-distribution-like (WDL) function [24–26] to investigate the ATI process of an atom in few-cycle laser pulses in the framework of the strong-field approximation (SFA). It is worthwhile mentioning that the SFA is accurate for a short-range system, e. g., negative ion, so it is suitable to investigate the validity of the semiclassical picture or the principle of the original attoclock technique scheme in which the Coulomb potential is ignored in the first place. The WDL function enables us to calculate the time-emission angle distribution, angular distribution and ionization time distribution of the ATI process of atom in elliptically and circularly polarized laser pulses with different carrier-envelope phases (CEPs). Then we explicitly and rigorously check the validity and accuracy of the attosecond angular streaking technique by comparing the quantum distributions with results given by the semiclassical simulation. Moreover, we also calculate the time-energy distribution and ionization time distribution of atoms in linearly polarized laser pulses and compare with semiclassical simulations to further systematically check the accuracy of the semiclassical picture in description of the photoionization process. Furthermore, we consider the non-adiabatic effect by performing calculation with PPT theory. The result shows that the non-adiabatic effect indeed reduces the discrepancy between semiclassical and quantum distributions and improves the accuracy of the attoclock technique.

THEORY AND NUMERICAL METHODS

The Wigner-distribution-like function derived from the strong-field approximation model is defined as (see [24] for more details):

$$f(t, \frac{p^2}{2}) = \frac{1}{\pi} \int_{-\infty}^{\infty} S'^*(t+t') S'(t-t') e^{-2i\frac{p^2}{2}t'} dt'. \quad (1)$$

where S' is given by

$$S' = \frac{\sqrt{2\pi}}{\sqrt{v}} \frac{\partial \phi_i(\mathbf{q})}{\partial \mathbf{q}} \cdot \mathbf{E}(t) \times \exp \left\{ i \int_{-\infty}^t [\mathbf{p} \cdot \mathbf{A}(\tau) + \frac{\mathbf{A}^2(\tau)}{2}] d\tau + i I_p t \right\}. \quad (2)$$

Here, v is normalization volume, $\mathbf{E}(t)$ the electric field and I_p the ionization potential of the atom. $\phi_i(\mathbf{q})$ is the Fourier transform of the atomic ground state $|\varphi_0\rangle$ and $\mathbf{q} \equiv \mathbf{p} + \mathbf{A}(t)$.

In this paper, we consider a laser pulse with a \sin^2 -type temporal envelop. The vector potential is given by

$$\mathbf{A}(t) = -\frac{E_0}{\omega} \sin^2 \left[\frac{\omega t}{n} \right] \left[\cos \frac{\theta}{2} \cos(\omega t + \varphi) \mathbf{e}_x - \sin \frac{\theta}{2} \sin(\omega t + \varphi) \mathbf{e}_y \right], \quad (3)$$

where E_0 is the peak field strength, ω the laser frequency, and $n/2$ the number of optical cycles contained in the laser pulse. φ is the initial carrier envelop phase (CEP). \mathbf{e}_x and \mathbf{e}_y are the unit vectors along the x and y axes, respectively. $\epsilon = \cot \frac{\theta}{2}$ is the ellipticity. The major axis is y-axis.

For simplification, here we only consider the distribution of electrons emitted in the polarization plane for a three-dimensional system. For a fixed kinetic energy $\frac{p^2}{2}$ in the polarization plane, the electron emission angle Θ varies from 0 to 2π , where Θ is the angle between the final momentum of electrons and x axis. From Eq. (2), we can find that S' is a function of momentum \mathbf{p} , which can be written as a function of two scalar variables p and Θ in a two-dimensional model. Here p is the absolute value of the electron momentum vector. Therefore, the formula of the Wigner-distribution-like function for a two-dimensional system can be written as following:

$$f(t, \frac{p^2}{2}, \Theta) = \frac{1}{\pi} \int_{-\infty}^{\infty} S'^*(t+t', \Theta) S'(t-t', \Theta) e^{-2i\frac{p^2}{2}t'} dt'. \quad (4)$$

The time-angle distribution function is given by

$$f'(t, \Theta) = \int f(t, \frac{p^2}{2}, \Theta) d(\frac{p^2}{2}). \quad (5)$$

Then one can find that the ionization probability as functions of time and emission angle can be given by

$$P(t) = \int f'(t, \Theta) d\Theta. \quad (6)$$

and

$$W(\Theta) = \int f'(t, \Theta) dt. \quad (7)$$

RESULTS AND DISCUSSIONS

In this paper, we consider H atoms ionized by a 6-cycle elliptically polarized laser field with peak intensity of 1×10^{14} W/cm² and ellipticity $\epsilon = 0.882$. It is worthwhile mentioning that all integrations are performed numerically in our quantum calculations.

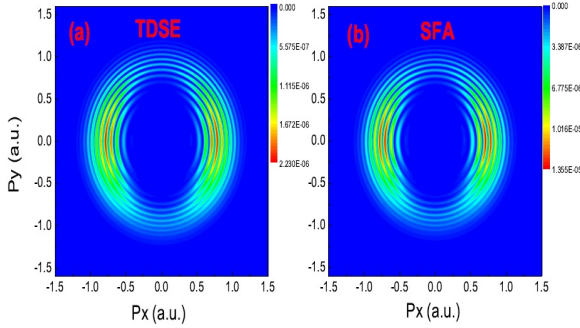


FIG. 1: Momentum spectra calculated by TDSE (a) and SFA (b) methods.

At first, we show the comparison of momentum spectra given by numerical solution of time-dependent Schrödinger equation (TDSE) (for details, see [27, 28]) and the SFA theory with the laser parameters of the CEP $\varphi = 0.5\pi$ and $\omega = 0.05691$ a.u. in Fig. 1. The short-range potential of $V = -A \frac{e^{-\kappa r}}{r}$ is adopted with $\kappa = 1$ in the TDSE method, where the value of A is taken as 1.90847 in order to make the model potential have the ground state energy of -0.5 a.u.. The momentum spectra in Fig. 1 show distinct ATI rings and are in good agreement with each other.

Elliptical and circular polarization

The semiclassical method in this paper is based on the ADK model [29–31] without taking into account the ionic Coulomb potential, which corresponds to the SFA model considered in our WDL calculation. The ionization rate in the semiclassical result is obtained using Eq. (21) of [32] with the Coulomb correction factor removed. The distribution of the initial momentum at the tunnel exit is

$P(p_{0\perp}, p_{0\parallel}) \propto \exp(-\frac{p_{0\perp}^2}{|E(t)|}) \exp(-\frac{p_{0\parallel}^2}{|E(t)|})$ ($E(t)$ is the laser field amplitude at time t . $p_{0\parallel}$ and $p_{0\perp}$ are the initial momenta parallel and vertical to the direction of the laser field polarization, respectively) [29]. When only initial transverse momentum is considered, we have $p_{0\parallel} = 0$. For clarity, we label the two different semiclassical methods according to the different initial momentum adopted as ADK_{\perp} with only the initial transverse momentum considered and $\text{ADK}_{\perp, \parallel}$ with both the initial transverse and longitudinal momenta considered.

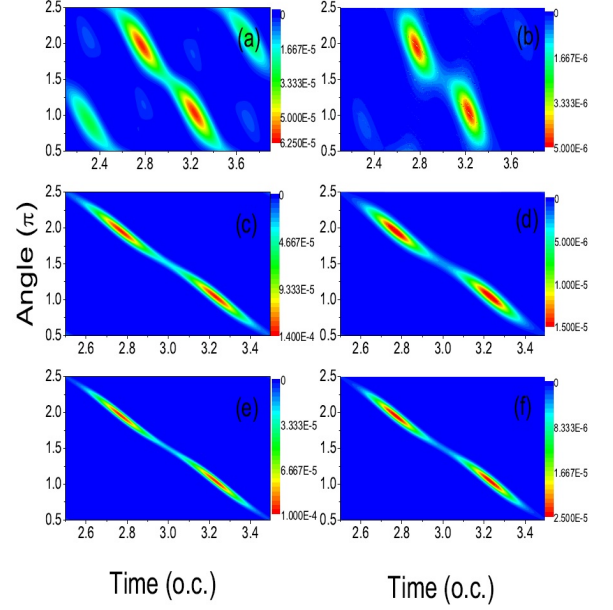


FIG. 2: Time-emission angle distributions in a 6-cycle laser pulse with the CEP $\varphi = 0.5\pi$ for different laser frequencies $\omega = 0.182$ a.u. ((a) and (b)), 0.05691 a.u. ((c) and (d)) and 0.03502 a.u. ((e) and (f)). Peak intensity $I = 1 \times 10^{14}$ W/cm² and the ellipticity $\epsilon = 0.882$. Quantum results: (a), (c), and (e); calculations of the semiclassical theory with $\text{ADK}_{\perp, \parallel}$: (b), (d), and (f).

Figure 2 shows the calculation of the time-emission angle distribution for H atoms in a 6-cycle laser pulse with the CEP $\varphi = 0.5\pi$ for three different optical frequencies. The distributions in Fig. 2 are obtained by Eq. (5) (see Figs. 2(a), 2(c), and 2(e)) and by semiclassical theory with $\text{ADK}_{\perp, \parallel}$ (see Figs. 2(b), 2(d), and 2(f)), respectively. For the semiclassical calculation obtained by $\text{ADK}_{\perp, \parallel}$, all distributions with different laser frequencies look similar—two main peaks located at $[\Theta, t] \sim [0(2\pi), 2.75 \text{ o.c.}]$ and $[\pi, 3.25 \text{ o.c.}]$ (o.c. is the abbreviation of optical cycle) and two additional small peaks at $t \sim 2.3$ and 3.7 o.c. (not shown in Fig. 2(d) and 2(f)) which correspond to the secondary peaks of the field amplitude. This is expectable since the ionization is independent of the frequency in the quasistatic tunneling picture. In contrast, for the quantum calculation, the time-emission

angle distributions show a clear transition with decreasing the laser frequency. For $\omega=0.182$ a.u. ($\gamma=3.4$), the distribution (Fig. 2(a)) is similar to the structure of the semiclassical calculation (Fig. 2(b)). When the laser frequency further decreases to $\omega=0.05691$ a.u. ($\gamma=1.07$) and 0.035 a.u. ($\gamma=0.66$), the quantum results more and more mimic the semiclassical results. Therefore, Fig. 2 demonstrates a transition from the multiphoton regime to the tunneling regime in the elliptically polarized laser field, which is consistent with the case of linearly polarized laser fields [25]. It is worthwhile mentioning that the time-emission angle distribution is also calculated using ADK_\perp method, however, the width is much narrower than the quantum result and is hardly dependent on the laser frequency (not shown here), indicating that the initial longitudinal momentum is an important non-adiabatic effect even in the tunneling regime.

To investigate quantitatively the accuracy of the semiclassical theory and validity of the attoclock technique, we then calculate the angular distribution $W(\Theta)$ by integrating the time-emission angle distribution over time t [33] and compare the quantum calculations with the semiclassical ones (see Fig. 3). All the angular distributions calculated by the semiclassical model $\text{ADK}_{\perp,\parallel}$ (dashed dotted lines) show a double-peak structure, which is symmetrical with respect to the angle $\Theta=1.5\pi$, in accordance with those shown in Figs. 2(b), 2(d), and 2(f). However, the widths of the angular distributions become progressively broader with the increasing frequency. We also give the results obtained by ADK_\perp (dotted lines), which also display a symmetric double-peak. The distinct feature different from the distribution gained by $\text{ADK}_{\perp,\parallel}$ is that the width of the angular distribution hardly depends on the frequency. By comparing between these two kinds of ADK calculations, we can infer that the initial longitudinal momentum distribution can cause broader width of the angular distribution, resulting in the difference between these two ADK calculations. This difference becomes larger when the frequency increases.

Similar to Fig. 2, the quantum calculation also clearly shows a transition from the multiphoton regime to the tunneling regime with decreasing laser frequency comparing with the semiclassical calculation. For $\omega=0.182$ a.u., the angular distribution in the quantum calculation shows a double-peak pattern with peak positions close to the semiclassical distribution obtained by $\text{ADK}_{\perp,\parallel}$ (see Fig. 3(a)). When the frequency decreases further, the quantum distribution becomes gradually close to the semiclassical calculations (see Figs. 3(b) and (c)). However, the widths of the quantum distributions are wider than the semiclassical ones and positions of peaks in the quantum and semiclassical calculations are still noticeable different (Here, we define the difference between the peak positions in the angular distributions calculated by the quantum theory and other methods (e.g. ADK models and non-adiabatic calculation mentioned below) as

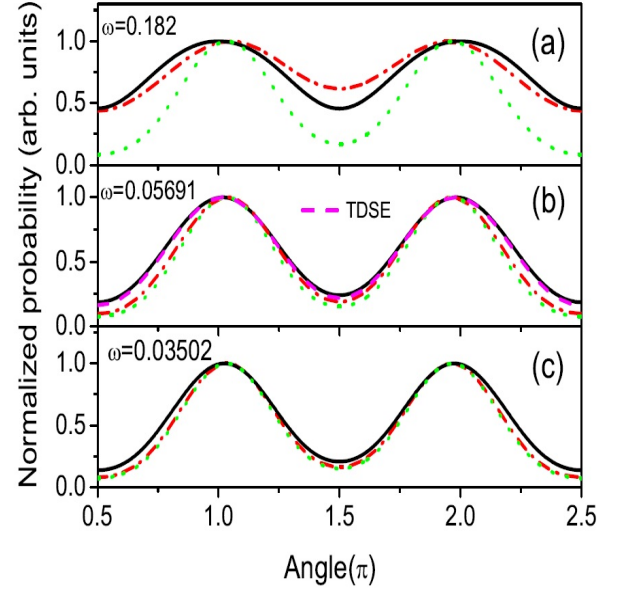


FIG. 3: Angular distributions calculated by the quantum theory (solid lines) and semiclassical theories with $\text{ADK}_{\perp,\parallel}$ (dashed dotted lines) and ADK_\perp (dotted lines) for different laser frequencies with the same parameters as those in Fig. 2. The angular distribution given by the TDSE for $\omega=0.05691$ a.u. is also present for comparison.

offset angle denoted by $\Delta\Theta$). The angular distribution gained by TDSE is also given in Fig. 3(b), which almost coincides with the curve of SFA model. The reason that the curves of the angular distributions calculated by TDSE and SFA models do not completely overlap is that the potential used in the TDSE calculation still possesses a finite range. Moreover, the effect of the initial longitudinal momentum of the photoelectron, which is considered as the non-adiabatic effect in the tunneling ionization process [19, 34, 35] can also be clearly seen in Fig. 3. For the lowest frequency $\omega=0.03502$ a.u., the two different semiclassical calculations (ADK_\perp and $\text{ADK}_{\perp,\parallel}$) can hardly be distinguished. For $\omega=0.05691$ a.u., the distribution of $\text{ADK}_{\perp,\parallel}$ becomes wider than that of ADK_\perp and is closer to the quantum distribution. The difference between two semiclassical calculations becomes larger when the frequency increases to $\omega=0.182$ a.u., however, the distribution of $\text{ADK}_{\perp,\parallel}$ becomes even wider than the quantum distribution. This is understandable since it is already in the multiphoton regime ($\gamma=3.4$), the non-adiabatic effect cannot be treated properly by the semiclassical model.

Moreover, we calculate the ionization time distribution $P(t)$ by integrating the time-emission angle distribution over angle Θ and the results are depicted in Fig. 4. For the semiclassical simulation, the ionization time distributions obtained by both $\text{ADK}_{\perp,\parallel}$ and ADK_\perp are the same since the initial momentum distributions in two calcula-

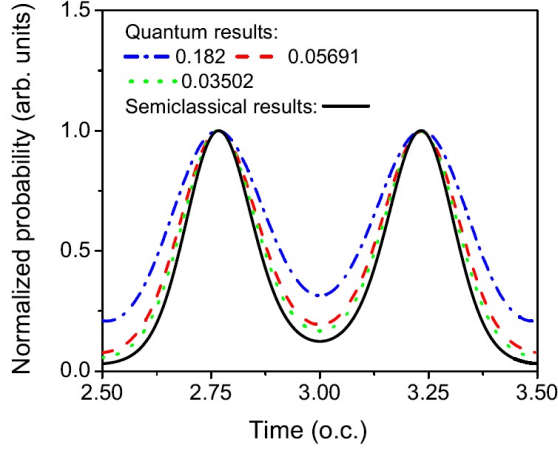


FIG. 4: Ionization time distributions calculated by the quantum theory and semiclassical theories with $\text{ADK}_{\perp,\parallel}$ and ADK_{\perp} (solid line) for different laser frequencies with the same parameters as those in Fig. 2.

tions are both normalized. Furthermore, it is expected that the ionization probability is only dependent on the electric field strength but independent of the laser frequency. As shown in Fig. 4, the ionization time distributions obtained by the semiclassical methods (black solid line) exhibit a double-peak structure for the time range from $t = 2.5$ to 3 o.c. and are indeed independent of the laser frequency, whose peak positions correspond to the maxima of the electric field strength ($t=2.76746$ and 3.23254 o.c.). For the quantum calculation, the distribution varies with the frequency. All ionization time distributions possess a double-peak structure and the widths of the peaks decrease with decreasing laser frequencies, becoming more and more close to the semiclassical results. However, the difference between the positions of peaks in the ionization time distributions calculated by the quantum method and semiclassical model still exists (for more details, see Fig. 5). We define this difference in the ionization time distribution as offset time denoted by Δt .

It should be noted that, for such wide frequency regime considered here which covers from tunneling to multi-photon regime, a theory including non-adiabatic effect should be used for calculations of both the angular and ionization time distributions. These calculations will be shown in Fig. 5 but here we only show the results of the adiabatic theory for comparison with the quantum result to show clearly approach of the quantum result to the semiclassical calculation with decreasing the frequency.

In order to show the offset angle and offset time more clearly, we zoom in one of two peaks in the angular and ionization time distributions. Figs. 5(a)-5(c) show the angular distributions for $\omega=0.182$ a.u., 0.0569 a.u. and 0.03502 a.u., respectively. As shown in Figs. 5(a)-5(c), it

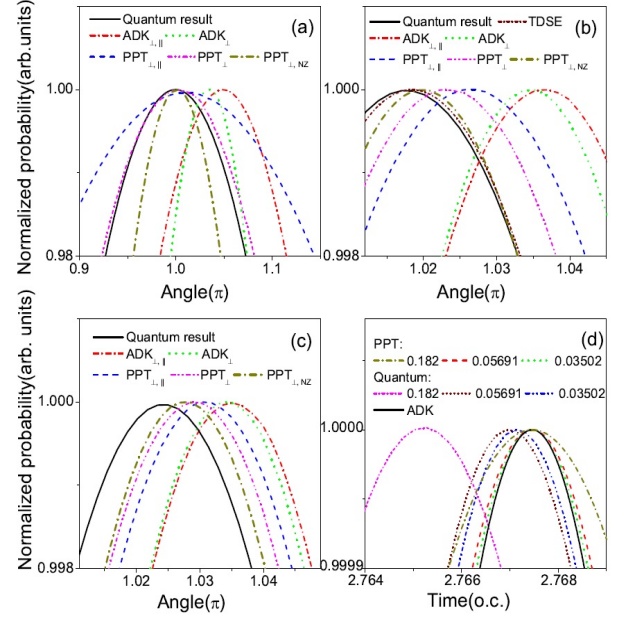


FIG. 5: Angular distributions calculated by the quantum, semiclassical and PPT theories for different laser frequencies $\omega = 0.182$ a.u. (a), $\omega = 0.05691$ a.u. (b) and $\omega = 0.03502$ a.u. (c); (d): ionization time distributions calculated by different methods (see text).

can be clearly seen that the widths of the angular distributions calculated by $\text{ADK}_{\perp,\parallel}$ (red dashed dotted lines) are broader than those gained by ADK_{\perp} (green dotted lines) and the peak position for $\text{ADK}_{\perp,\parallel}$ is a little farther from the quantum peak position comparing with ADK_{\perp} calculation. These differences between two ADK calculations result from the initial longitudinal momentum as mentioned above. When the frequency decreases, these differences also decrease, which can be attributed to relatively larger momentum of the electron acquired from the laser field with lower frequency comparing with the wavelength-independent initial momentum of the electron at the tunnel exit [29–31]. It is well-known that the semiclassical model is only valid in the quasistatic tunneling regime. Here, we also consider the non-adiabatic effect using PPT theory [36, 37]. The ionization rates for PPT are obtained by Eqs. (3.4)-(3.6) of [36]. The pre-exponential factor is taken from Eq. (59) of [37]. The initial momentum at the tunnel exit is also taken into account in the same way as that in the semiclassical model as mentioned above for an explicit comparison with the semiclassical calculation. The PPT calculations including the only initial transverse momentum and both the initial transversal and longitudinal momenta at tunnel exit are denoted as PPT_{\perp} and $\text{PPT}_{\perp,\parallel}$, respectively. From Figs. 5(a)-5(c), we can find that the peak width of $\text{PPT}_{\perp,\parallel}$ (dashed line) is also broader than that ob-

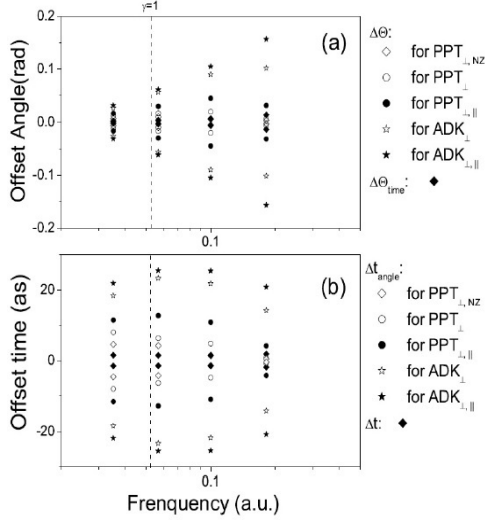


FIG. 6: $\Delta\Theta$, $\Delta\Theta_{time}$ (a) and Δt , Δt_{angle} (b) obtained by the different methods as shown in Fig. 5 for four laser frequencies. $\Delta\Theta_{time}$ (Δt_{angle}) means the angular (ionization time) offset transformed from the offset time (angle) (see text).

tained by PPT_{\perp} (dashed dotted dotted line) and the peak position of the latter one is closer to the quantum peak position than the former one, which are similar to the differences between $ADK_{\perp,\parallel}$ and ADK_{\perp} results. Furthermore, we also consider initial transverse momentum with nonzero maximum in the PPT theory (denoted by $PPT_{\perp,NZ}$ as shown in Figs. 5(a)-5(c)). The nonzero peak of the transverse momentum is given by $P_{\perp} = \epsilon\gamma(t)\sqrt{2I_p}/6$ (here, $\gamma(t) = \sqrt{2I_p\omega}/|E(t)|$ and ϵ is the ellipticity) [23]. It can be seen that the peak position is closer to that of the quantum result than PPT_{\perp} in the angular distribution. Comparing the PPT calculations with the ADK results, it can be seen that the peak positions calculated by PPT are closer to those of the quantum theory, indicating that the non-adiabatic effect can reduce the offset angle. It is worthwhile mentioning that for the lower frequencies $\omega = 0.05691$ and 0.03502 a.u., the widths of the angular distributions of PPT theory are closer to the distributions of the quantum theory than the results of semiclassical theory. However, for $\omega = 0.182$ a.u., the angular distributions calculated by the PPT theory are even broader than the distribution of the quantum theory, which can also be seen clearly in Fig. 5(a). This indicates that the PPT theory is invalid in the multiphoton regime. It should be noted that for $\omega = 0.05691$ in Fig. 5(b), although there is a slight offset angle between the SFA and TDSE results due to a finite range of the potential used in the TDSE calculation, the value of offset angle is significantly smaller than any values of other offset angles under the same frequency condition. This implies that the calculation based on the SFA is accurate enough.

For the ionization time distribution (see Fig. 5(d)), the peak position of the semiclassical theory (black solid line) corresponds to the maximal field strength. For the quantum calculations, not only the peak width (shown clearly in Fig. 4 but also the peak position varies with frequency, which becomes more and more close to those obtained by the semiclassical theory (see Fig. 5(d)) when the frequency decreases. For the PPT theory, although the peak widths of the ionization time distributions for three frequencies are different and become more and more broad with increasing frequencies, the peak positions are the same as those of the semiclassical theory and are independent of the laser frequency, which means that the value of the offset time between the quantum and ADK calculations is the same as that between the quantum and PPT calculations for a given laser frequency. As shown in Fig. 5(d), when the frequency decreases, the ionization time distribution approaches the semiclassical results, which can be attributed to that the non-adiabatic effect is less and less important with decreasing Keldysh parameter.

Figure 6 shows the values of the offset angles (Fig. 6(a)) and offset times (Fig. 6(b)) extracted from Fig. 5. The offset angles or times are positive and negative, corresponding to the left and right peaks exhibited in Figs. 3 and 4, respectively. In order to investigate the correspondence between the offset angle and the offset time, we also give the corresponding offset angle calculated from the offset time Δt by the relation $\omega\Delta t = \Theta$. Here we define this angular offset as $\Delta\Theta_{time} = 2\pi\Delta t$ (Δt in units of o.c.). Similarly, we define the corresponding offset time transformed from the offset angle $\Delta\Theta$ in the angular distribution as Δt_{angle} ($\Delta t_{angle} = \frac{\Delta\Theta}{2\pi}$). Fig. 6(a) shows the offset angles $\Delta\Theta$ and $\Delta\Theta_{time}$ for four different frequencies (the result of $\omega = 0.1$ a.u. is also shown here to exhibit the frequency dependence of the offset time and angle more clearly). One can find that the offset angles $\Delta\Theta$ of ADK_{\perp} , $ADK_{\perp,\parallel}$, PPT_{\perp} and $PPT_{\perp,\parallel}$ are always larger than $\Delta\Theta_{time}$ for all frequencies except $\Delta\Theta$ of PPT_{\perp} for $\omega = 0.182$ a.u. Moreover, the offset angle of $PPT_{\perp,NZ}$, which is smaller than the other four offset angles as mentioned before, is still larger than $\Delta\Theta_{time}$ in the tunneling ($\gamma \ll 1$) and nonadiabatic regimes ($\gamma \approx 1$) but becomes almost equal to or even smaller than $\Delta\Theta_{time}$ in the multiphoton regime.

Figure 6(b) depicts the offset time Δt and Δt_{angle} in units of attosecond (as). Some interesting features can be found in Fig. 6(b). The offset time hardly depends on the frequency. When the frequency decreases from 0.182 a.u. to 0.03502 a.u., the offset time Δt only changes from about 1.8 as to 1.5 as. However, the corresponding offset time Δt_{angle} varies in a much large range from 0.44 as to 26 as. Generally, the offset time Δt_{angle} of the PPT theory is considerably smaller than that of the ADK theory, indicating that the non-adiabatic effect will indeed reduce the discrepancy between the quantum and semiclassical

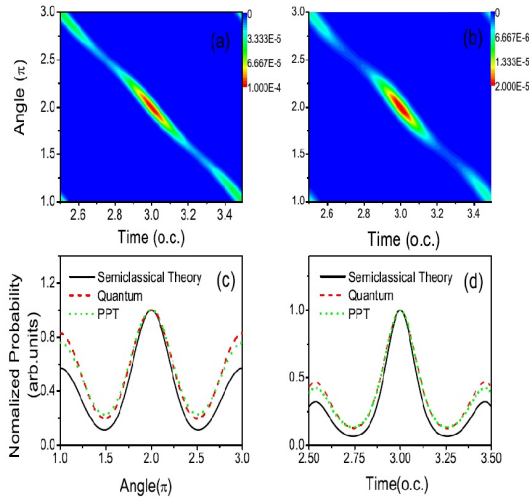


FIG. 7: Time-angle distributions calculated by the quantum theory (a) and the semiclassical theory with ADK_{⊥,||} (b) for $\omega=0.05691$ a.u.. Angular distribution (c) and ionization time distribution (d) obtained by both the quantum and semiclassical methods. The parameters are the same as those of Fig. 3(c) except CEP $\varphi = 0$.

calculations. However, it can be clearly seen that, except for the calculations of PPT_⊥ and PPT_{⊥,NZ} in the multiphoton regime ($\omega = 0.1$ and 0.182 a.u.), the offset times Δt are noticeably smaller than the corresponding offset times Δt_{angle} transformed from the offset angle in the angular distribution. This result implies that the offset angle $\Delta\Theta$ in the angular distribution *does not* correspond to the offset time Δt in the ionization time distribution. So the "attoclock" measurement [8] which relies on the correspondence between the offset angle and time is in principle inaccurate. It is noteworthy that there is a debate on whether the non-adiabatic effect is responsible for the offset angle measured for He in the experiment [11, 14]. Our calculation shows that although the non-adiabatic effect taken into account in the PPT theory can reduce the value of the offset angle, the offset angle between the quantum and PPT calculations still does not correspond to the offset time between these two calculations, which indicates that the discrepancy between the two kinds of offsets cannot be attributed to the non-adiabatic effect [16–18].

It is worthwhile mentioning that for pulses with CEP $\varphi = 0.5\pi$, because the two peaks in the angular (ionization time) distribution are symmetric, the absolute values of the offset angles (times) for the two peaks are equal. For other CEPs, the two peaks in the angular (ionization time) distribution become asymmetric and the absolute values of the offsets for these two peaks are not equal. Another special case is CEP $\varphi = 0$ (see Fig. 7). In this case, the maximal ionization rate occurs at the center of

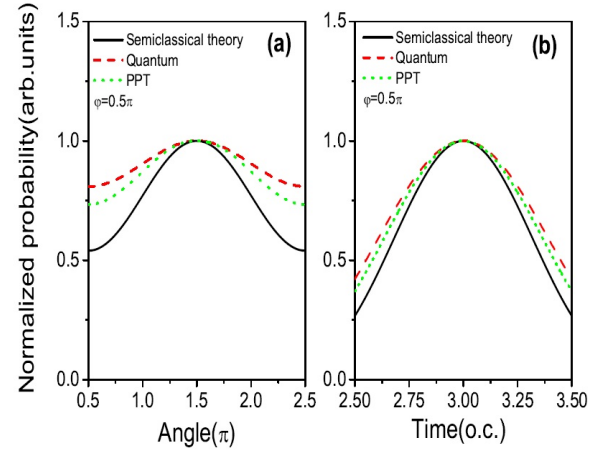


FIG. 8: Angular (a) and ionization time (b) distributions obtained by the quantum and semiclassical methods for circularly polarized laser pulses. The other parameters are the same as those of Fig. 7.

the laser pulse at $t = 3$ o.c. as shown in Fig. 7. Figs. 7(a) and 7(b) are the time-emission angle distributions calculated by the quantum theory and the semiclassical theory with ADK_{⊥,||}, respectively. Both distributions show one main peak located at $[\Theta, t] \sim [0(2\pi), 3 \text{ o.c.}]$ and two other peaks at $t \sim 2.536$ and 3.464 o.c. Moreover, the angular distribution and the ionization time distribution are given in Figs. 7(c) and 7(d), respectively. The non-adiabatic effect is also considered by PPT theory and the corresponding results are given in Figs. 7(c) and 7(d). As displayed in Fig. 7(c), all the angular distributions obtained by the quantum theory, semiclassical theory and PPT theory show two asymmetric peaks: one higher peak (namely one main peak) at emission angle $\Theta = 2\pi$ and one lower peak at emission angle $\Theta = \pi(3\pi)$. The peak positions of the two peaks calculated by these three methods coincide with each other, which means that the offset angle for the both higher peak and lower peak are all zero $\Delta\Theta = 0$. However, the ionization time distributions show a three-peak structure. For the highest peak at $t = 3$ o.c. which corresponds to the maximal field of the laser pulse, the offset time Δt is zero. For the other two peaks on the two sides of the highest peak, these peaks are symmetric with respect to the center of the pulse $t = 3$ o.c. and the absolute values of the offset times are equal $|\Delta t| = 0.004$ o.c. (see Fig. 7(d)). As shown in Figs. 7(c) and 7(d), when the non-adiabatic effect is considered, the widths of both the angular distribution and the ionization time distribution are closer to the quantum distributions than the ADK results, however, the positions of the peaks remain the same as those of the ADK calculations. In addition, the calculations for circularly polarized laser pulses are shown in Fig. 8. In this case, there is only one peak in both the angular and ionization time distributions and

the peak positions both coincide with the ADK (solid line) and PPT (dotted line) calculations, in agreement with the results of Torlina *et al.* [15] and Ni *et al.* [38].

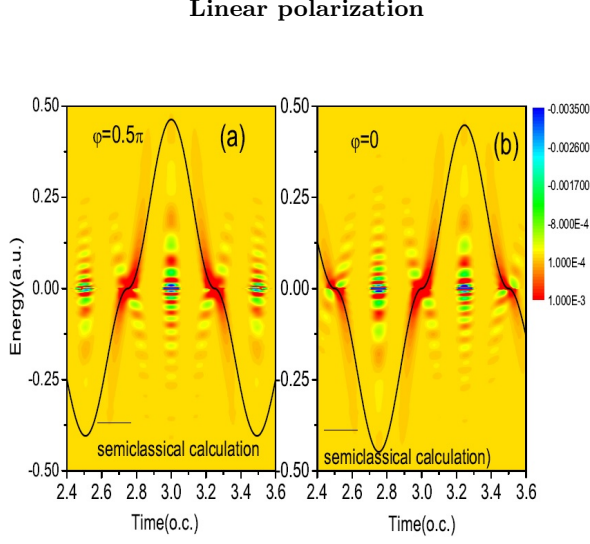


FIG. 9: Time-energy distribution of photoelectron in linearly polarized laser pulse. Here positive and negative energies indicate the emission directions of the photoelectron. (a): CEP $\varphi = 0.5\pi$; (b): CEP $\varphi = 0$. The other parameters are the same as those of Fig. 7. The prediction of the simpleman's model is also shown (see text).

To systematically investigate the accuracy of the semiclassical model, we also calculate photoionization process of atoms in linearly polarized laser pulses. The time-energy distributions of H atoms in an 800 nm 6-cycle laser field with peak intensity of 1×10^{14} W/cm² and CEPs of 0.5π and 0 are depicted in Fig. 9. For comparison, the prediction of the simpleman's model is also shown in Fig. 9. In agreement with Fig. 2 of [25], the correspondence between the instant of ionization and the final kinetic energy (represented by strips in Fig. 9) is just qualitatively consistent with the simpleman's prediction. Although the maximum of the strips is close to the semiclassical calculation near zero energy, two calculations diverge with increasing energy still.

In Fig. 10, we show the ionization time distributions of both quantum and semiclassical calculations. The results are similar to the elliptical polarization case. For CEP $\varphi = 0.5\pi$, two peaks of both calculations are symmetric and the offset times are also symmetric ($\Delta t = \pm 32$ as). While for $\varphi = 0$, the higher central peaks of two calculations coincide with each other but the lower side peaks show noticeable offsets ($\Delta t = \pm 29$ as). The PPT calculations are also given in Fig. 10 (dotted lines). The peak positions for PPT theory are the same as those for semiclassical calculations and the peak widths are broader than the semiclassical distribution, which is similar to the

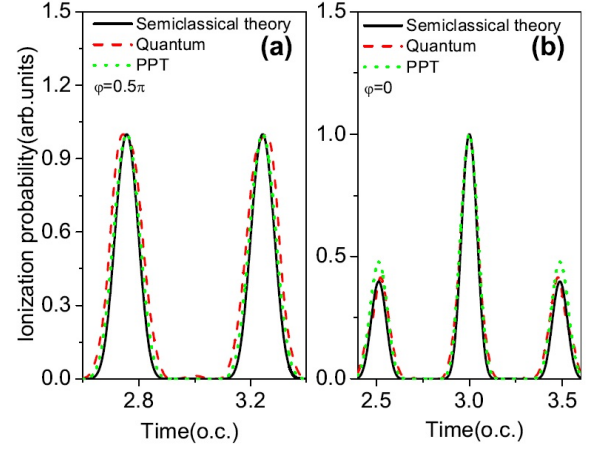


FIG. 10: Ionization time distribution of photoelectron in the linearly polarized laser pulses. (a): CEP $\varphi = 0.5\pi$; (b): CEP $\varphi = 0$. The other parameters are the same as those of Fig. 7.

case of the elliptical polarization. It is noteworthy that the offset time in the linearly polarized case is considerably larger than that in the elliptically polarized laser field.

Discussion

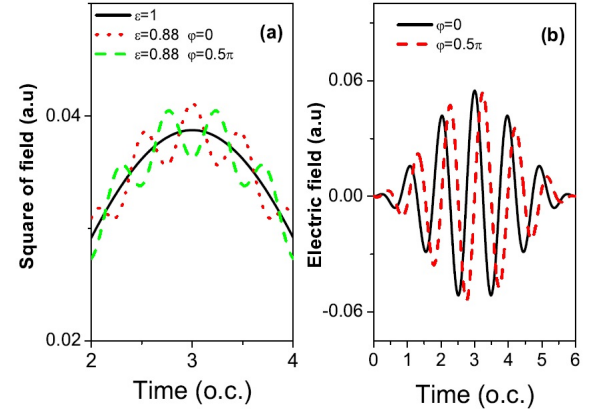


FIG. 11: (a): Square of electric field of elliptically and circularly polarized laser pulses. (b): Electric field of linearly polarized laser pulses for $\varphi = 0$ and 0.5π .

In the Wigner-distribution-like function, to obtain the ionization time distribution in the quantum theory, correlation effect must be taken into account. The ionization probability at moment t is integration of the correlation between the ionization at $t + t'$ and $t - t'$ where t' goes over the whole laser pulse, which means that the quantum process is temporally nonlocalized. In contrast, the ionization process in the semiclassical picture is tempo-

rally localized, viz., ionization at one moment is independent of ionization at other moment. Therefore, the semiclassical theory is an approximate description of the photoionization process and, as shown by our calculation, is usually not quantitatively consistent with the quantum calculation. The coincidence of the two calculations in some specific cases is actually accidental and can be attributed to the time-reverse invariant symmetry of the laser field. For an elliptically laser pulse with CEP $\varphi = 0$ or a circularly polarized laser pulse with any CEP, the laser field possesses time-reverse invariant symmetry with maximum at the center of the laser pulse as shown in Fig. 11. Therefore, the ionization time and angular distributions are symmetrical and the positions of the peaks (the higher peak in the elliptically polarized case with $\varphi = 0$), which are generated at the maximum of the laser field, are independent of the calculation method. For CEP $\varphi = 0.5\pi$, though the laser field is also time-reverse invariant, this symmetry cannot ensure the coincidence between the peaks of different calculation methods but guarantee that the offsets of the two symmetrical peaks in both the ionization time and angular distributions are symmetrical (positive and negative but the absolute values are the same, see. Figs. 3- 6). Moreover, as mentioned before, the lower peaks in the angular distribution for two calculations also coincide with each other in the $\varphi = 0$ case (see Fig. 7(c)). This is because that the lower peak in the angular distribution is actually composed of two halves symmetrical with respect to $\Theta = \pi$ which are generated by two symmetrical peaks with respect to $t=3$ o.c. in the ionization time distribution (see Fig. 7(d)) and this symmetry is independent of the calculation method. In the linearly polarized cases, the offset time in the linearly polarized case is considerably larger than that in the elliptically polarized laser field. This can be attributed to stronger correlation effect in the linearly polarized laser field since in this case, the emitted photoelectrons concentrate more in one direction (laser field direction) than that in the elliptically polarized field. For other CEP, the time-reverse invariant is broken, hence the distributions are asymmetrical and the offsets are also asymmetrical. Moreover, our analysis indicates that neither the offset time nor the offset angle in the elliptically polarized laser field can be interpreted as the tunneling time delay. These offsets, together with the widths of the peaks in the distributions, however, could be taken as effective measures for the validity of the semiclassical theory in description of the ionization process in the laser field.

CONCLUSION

The WDL function enables us to obtain the time-emission angle distribution, angular distribution and ionization time distribution of atoms in the elliptically polar-

ized laser fields and time-energy distribution and ionization time distribution of atoms in the linearly polarized laser fields. Comparison shows that these distributions are usually not in quantitative agreement with the semiclassical model calculation except in some specific cases. Discrepancy between two calculations can be attributed to correlation effect or temporal nonlocalization characteristic of quantum mechanics and coincidence between two calculations in some specific cases is due to temporal symmetry of the laser pulse. Moreover, we find that the offset angle are generally not consistent with the offset time even when the non-adiabatic effect is taken into account, indicating that the attosecond angular streaking technique is in principle inaccurate. Our result clearly shows the applicability and limit of the technique, which is important for interpretation and understanding on relevant experimental and theoretical results.

Funding

This work was partially supported by the National Key program for S&T Research and Development (No. 2016YFA0401100), NNSFC (No. 11774361, 11775286, 11425414 and 11774215) and the Open Fund of the State Key Laboratory of High Field Laser Physics (SIOM).

-
- [1] P. Agostini, F. Fabre, G. Mainfray, G. Petite, and N. K. Rahman, "Free-free transitions following six-photon ionization of xenon atoms," *Phys. Rev. Lett.* **42**, 1127-1130 (1979).
 - [2] W. Becker, F. Grasbon, R. Kopold, D. B. Milošević, G. G. Paulus, and H. Walther, "Above-threshold ionization: From classical features to quantum effects," *Adv. At. Mol. Opt. Phys.* **48**, 35-98 (2002).
 - [3] L. V. Keldysh, "Ionization in field of a strong electromagnetic wave", *Sov. Phys. JETP*. **20**, 1307-1314 (1965).
 - [4] H. B. van Linden van den Heuvell and H. G. Muller, *Multiphoton Processes* edited by S. J. Smith and P. L. Knight (Cambridge University, Cambridge, UK, 1988), p. 25.
 - [5] P. B. Corkum, "Plasma perspective on strong-field multiphoton ionization," *Phys. Rev. Lett.* **71**, 1994-1997 (1993).
 - [6] F. Krausz and M. Ivanov, "Attosecond physics," *Rev. Mod. Phys.* **81**, 163-234 (2009).
 - [7] P. Eckle, M. Smolarski, P. Schlup, J. Biegert, A. Staudte, M. Schöffler, H. G. Muller, R. Dörner, and U. Keller, "Attosecond angular streaking," *Nat. Phys.* **4**, 565-570 (2008).
 - [8] P. Eckle, A. N. Pfeiffer, C. Cirelli, A. Staudte, R. Dörner, H. G. Muller, M. Büttiker, and U. Keller, "Attosecond ionization and tunneling delay time measurements in helium," *Science* **322**, 1525-1529 (2008).
 - [9] A. N. Pfeiffer, C. Cirelli, M. Smolariski, R. Dörner, and U. Keller, "Timing the release in sequential double ionization," *Nat. Phys* **7**, 428-433 (2011).

- [10] A. N. Pfeiffer, C. Cirelli, M. Smolarski, D. Dimitrovski, M. Abu-samha, L. B. Madsen, and U. Keller, "Attoclock reveals natural coordinates of the laser-induced tunnelling current flow in atoms," *Nat. Phys* **8**, 76-80 (2012).
- [11] R. Boge, C. Cirelli, A. S. Landsman, S. Heuser, A. Ludwig, J. Maurer, M. Weger, L. Gallmann, and U. Keller, "Probing nonadiabatic effects in strong-field tunnel ionization," *Phys. Rev. Lett.* **111**, 103003 (2013).
- [12] J. Wu, L. Ph. H. Schmidt, M. Kunitski, M. Meckel, S. Voss, H. Sann, H. Kim, T. Jahnke, A. Czasch, and R. Dörner, "Multiorbital tunneling ionization of the CO molecule," *Phys. Rev. Lett.* **108**, 183001 (2012).
- [13] A. S. Landsman, M. Weger, J. Maurer, R. Boge, A. Ludwig, S. Heuser, C. Cirelli, L. Gallmann, and U. Keller, "Ultrafast resolution of tunneling delay time," *Optica* **1**, 343-349 (2014).
- [14] I. A. Ivanov and A. S. Kheifets, "Strong-field ionization of He by elliptically polarized light in attoclock configuration," *Phys. Rev. A* **89**, 021402 (2014).
- [15] L. Torlina, F. Morales, J. Kaushal, I. Ivanov, A. Kheifets, A. Zielinski, A. Scrinzi, H. G. Muller, S. Sukiasyan, M. Ivanov, and O. Smirnova, "Interpreting attoclock measurements of tunnelling times," *Nat. Phys* **11**, 503-508 (2015).
- [16] G. L. Yudin and M. Y. Ivanov, "Nonadiabatic tunnel ionization: Looking inside a laser cycle," *Phys. Rev. A* **64**, 013409 (2001).
- [17] I. Barth and O. Smirnova, "Nonadiabatic tunneling in circularly polarized laser fields: Physical picture and calculations," *Phys. Rev. A* **84**, 063415 (2011).
- [18] C. Wang, X. Y. Lai, Z. L. Hu, Y. J. Chen, W. Quan, H. P. Kang, C. Gong, and X. Liu, "Strong-field atomic ionization in elliptically polarized laser fields," *Phys. Rev. A* **90**, 013422 (2014).
- [19] A. N. Pfeiffer, C. Cirelli, A. S. Landsman, M. Smolarski, D. Dimitrovski, L. B. Madsen, and U. Keller, "Probing the longitudinal momentum spread of the electron wave packet at the tunnel exit," *Phys. Rev. Lett.* **109**, 083002 (2012).
- [20] C. Hofmann, A. S. Landsman, C. Cirelli, A. N. Pfeiffer, and U. Keller, "Comparison of different approaches to the longitudinal momentum spread after tunnel ionization," *J. Phys. B: At. Mol. Opt. Phys* **46**, 125601 (2013).
- [21] N. I. Shvetsov-Shilovski, D. Dimitrovski, and L. B. Madsen, "Ionization in elliptically polarized pulses: Multi-electron polarization effects and asymmetry of photoelectron momentum distributions," *Phys. Rev. A* **85**, 023428 (2012).
- [22] C. Hofmann, T. Zimmermann, A. Zielinski, and A. S. Landsman, "Non-adiabatic imprints on the electron wave packet in strong field ionization with circular polarization," *New J. Phys* **18**, 043011 (2016).
- [23] M. Klaiber, K. Z. Hatsagortsyan, and C. H. Keitel, "Tunneling Dynamics in Multiphoton Ionization and Attoclock Calibration," *Phys. Rev. Lett.* **114**, 083001 (2015).
- [24] L. Guo, S. S. Han, and J. Chen, "Time-energy analysis of above-threshold ionization," *Opt. Express* **18**, 1240-1248 (2010).
- [25] L. Guo, S. S. Han, and J. Chen, "Time-energy analysis of above-threshold ionization in few-cycle laser pulses," *Phys. Rev. A* **86**, 053409 (2012).
- [26] L. Guo, S. S. Han, S. L. Hu, and J. Chen, "Time-energy analysis of above-threshold ionization in the transverse direction of the linearly polarized laser pulses," *J. Phys. B: At. Mol. Opt. Phys* **50**, 125006 (2017).
- [27] V. Mosert and D. Bauer, "Photoelectron spectra with Qprop and t-SURFF," *Comput. Phys. Commun.* **207**, 452-463 (2016).
- [28] L. Tao and A. Scrinzi, "Photo-electron momentum spectra from minimal volumes: the time-dependent surface flux method," *New J. Phys.* **14**, 013021 (2012).
- [29] X. L. Hao, W. D. Li, J. Liu, and J. Chen, "Effect of the electron initial longitudinal velocity on the nonsequential double-ionization process," *Phys. Rev. A* **83**, 053422 (2011).
- [30] T. Brabec, M. Y. Ivanov, and P. B. Corkum, "Coulomb focusing in intense field atomic processes," *Phys. Rev. A* **54**, R2551-R2554 (1996).
- [31] B. Hu, J. Liu, and S. G. Chen, "Plateau in above-threshold-ionization spectra and chaotic behavior in rescattering processes," *Phys. Lett. A* **236**, 533-542 (1997).
- [32] V. P. Krainov, "Ionization rates and energy and angular distribution at the barrier-suppression ionization of complex atoms and atomic ions," *J. Opt. Soc. Am. B* **14**, 425 (1997).
- [33] The angular distribution can also be calculated by the first order of the expansion of the S-matrix given in, for example, Reiss, H.R. Effect of an intense electromagnetic field on a weakly bound system. *Phys. Rev. A* **22**, 1786-1813 (1980).
- [34] N. Teeny, E. Yakaboylu, H. Bauke, and C. H. Keitel, "Ionization Time and Exit Momentum in Strong-Field Tunnel Ionization," *Phys. Rev. Lett.* **116**, 063003 (2016).
- [35] N. Camus, E. Yakaboylu, L. Fechner, M. Klaiber, M. Laux, Y. Mi, KZ Hatsagortsyan, T. Pfeifer, CH Keitel, and R. Moshammer, "Experimental evidence for quantum tunneling time," *Phys. Rev. Lett.* **119**, 023201 (2017).
- [36] V. S. Popov, "Tunnel and multiphoton ionization of atoms and ions in a strong laser field (Keldysh theory)," *Physics-Uspekhi* **47**(9), 855-885 (2004).
- [37] A. M. Perelomov, V. S. Popov, and M. V. Terentev, "Ionization of atoms in an alternating electric field," *J. Expt. Theoret. Phys* **50**, 1393-1409 (1966).
- [38] H. Ni, U. Saalman, and J. M. Rost, "Tunneling ionization time resolved by backpropagation," *Phys. Rev. Lett.* **117**, 023002 (2016).